PHYSICAL REVIEW B **102**, 161104(R) (2020)

Rapid Communications

Systematic comparison and cross-validation of fixed-node diffusion Monte Carlo and phaseless auxiliary-field quantum Monte Carlo in solids

Fionn D. Malone,[1,*] Anouar Benali,[2,*] Miguel A. Morales,[1] Michel Caffarel,[3] Paul R. C. Kent,[4] and Luke Shulenburger[5,†]

[1]*Quantum Simulations Group, Lawrence Livermore National Laboratory, 7000 East Avenue, Livermore, California 94551, USA*
[2]*Computational Science Division, Argonne National Laboratory, Argonne, Illinois 60439, USA*
[3]*Laboratoire de Chimie et Physique Quantiques, Université de Toulouse, CNRS, UPS, France*
[4]*Center for Nanophase Materials Sciences and Computational Sciences and Engineering Division, Oak Ridge National Laboratory, Oak Ridge, Tennessee 37831, USA*
[5]*HEDP Theory Department, Sandia National Laboratories, Albuquerque, New Mexico 87185, USA*

(Received 3 June 2020; revised 2 September 2020; accepted 17 September 2020; published 7 October 2020)

Quantum Monte Carlo (QMC) methods are some of the most accurate methods for simulating correlated electronic systems. We investigate the compatibility, strengths, and weaknesses of two such methods, namely, diffusion Monte Carlo (DMC) and auxiliary-field quantum Monte Carlo (AFQMC). The multideterminant trial wave functions employed in both approaches are generated using the configuration interaction using a perturbative selection made iteratively (CIPSI) technique. Complete basis-set full configuration interaction energies estimated with CIPSI are used as a reference in this comparative study between DMC and AFQMC. By focusing on a set of canonical finite–size solid-state systems, we show that both QMC methods can be made to systematically converge towards the same energy once basis-set effects and systematic biases have been removed. AFQMC shows a much smaller dependence on the trial wave function than DMC while simultaneously exhibiting a much larger basis-set dependence. We outline some of the remaining challenges and opportunities for improving these approaches.

DOI: 10.1103/PhysRevB.102.161104

Introduction. The accurate first-principles description of correlated materials is one of the grand challenges of chemistry, materials science, and physics [1]. Density functional theory [2,3] (DFT) is the workhorse of these communities, offering an often good enough accuracy relative to its computational cost. However, the use of DFT in practice suffers from a number of well-known deficiencies including uncertainty in the choice of exchange-correlation functional [4] and with the treatment of strongly correlated materials. While no single approach is likely to work well in every situation [5], complementary methods are desired that can be systematically converged and applied to novel materials in a fully *ab initio* manner [6]. Here we focus on quantum Monte Carlo (QMC) methods that can potentially achieve this goal.

Several different flavors of QMC exist. Generally, ground-state QMC methods use a direct wave-function-based approach to solving the many-electron Schrödinger equation and all use statistical methods to treat the high dimensionality of the many-electron problem efficiently. They make a few well-defined approximations that can in principle be systematically removed, albeit at an exponential cost in general. Diffusion Monte Carlo (DMC) [7] and auxiliary-field quantum Monte Carlo (AFQMC) [8–10] have emerged as the most reliable and general-purpose approaches capable of simulating models [11,12] to *ab initio* systems [13–22]. Both methods can be formulated to run efficiently on modern supercomputing architectures [23,24].

QMC methods also come with a number of drawbacks. They are expensive relative to DFT or even quantum chemistry approaches for small to moderately sized systems. They also suffer from finite-size effects common to all many-body techniques, which can be slow to converge. Most seriously, in order to achieve an algorithm that scales only polynomially with system size, both DMC and AFQMC employ constraints in the Monte Carlo sampling to avoid the fermion sign problem. This can introduce a significant bias. It is thus important to assess the quality of the approximations made in both DMC and AFQMC as they become more widely applied in challenging environments.

AFQMC and DMC share many similarities: they are projector methods, they use random walkers to sample the many-electron ground state, and they employ a constraint to control the fermion sign (phase) problem in DMC (AFQMC). It should be stressed that the nature of the two constraints is quite different [25]. The methods differ in several additional important ways. First, DMC has the significant advantage of working in real space and thus in the complete basis-set (CBS) limit. AFQMC works in a finite basis set constructed from plane waves [26,27], Kohn-Sham states [28,29], or a periodized local basis set [9,30,31]. Converging the AFQMC results with respect to the single-particle basis set in solid-state calculations introduces a considerable overhead. Second, DMC can incorporate Jastrow factors in the trial wave function to account for electron-electron cusp conditions and

---

[*] These authors contributed equally to this work.
[†] lshulen@sandia.gov

capture residual dynamic correlation. Incorporating Jastrow factors in AFQMC is a challenging prospect [32]. Finally DMC, in contrast to AFQMC [25], can be made fully variational in the energy, making the assessment and choice of improved trial wave functions straightforward in principle. As the longer established method, DMC has seen by far the widest range of application, including to bulk systems with over 1000 atoms [33,34] and to complex transition metal oxide heterostructures [35].

Despite the basis-set convergence challenges, AFQMC offers several promising features precisely because it works directly in an orbital basis. Namely, all-electron, frozen core, and nonlocal pseudopotential calculations can be performed without additional approximations. In contrast, DMC requires the use of approximations to evaluate nonlocal potentials, either the original nonvariational locality approximation [36] or more recent T-moves methods [37] that restore the variational property and increase stability. The inclusion of spin-orbit effects in AFQMC is straightforward requiring very few algorithmic modifications [38]. Furthermore, many developments from the quantum chemistry community can be used to improve AFQMC, such as the use of tensor hypercontraction approaches [30,39–45]. Properties other than the total energy can be more directly accessed [46–50]. Finally, a growing body of literature suggests that single-determinant AFQMC is often more accurate than single-determinant DMC [11–13]. However, little research has been dedicated to the direct comparison between the two methods in solids and application of multiple determinants.

In this Rapid Communication we show that both AFQMC and DMC can be made to converge towards the same correlation energy for simple finite-size solids. By employing multideterminant wave functions we show that AFQMC converges more rapidly to the exact ground-state energy than DMC does. DMC, on the other hand, shows only a weak basis-set dependence. We close by offering some insight into the future prospects and challenges for the methods.

Methods. Both AFQMC and DMC are projector QMC methods wherein the ground state, $|\Psi_0\rangle$, of the many-electron Hamiltonian, $\hat{H}$, is determined by

$$|\Psi_0\rangle \propto \lim_{\tau\to\infty} \exp(-\tau\hat{H})|\Phi_0\rangle = \lim_{\tau\to\infty} \hat{P}(\tau)|\Phi_0\rangle, \quad (1)$$

where $|\Phi_0\rangle$ is some initial state satisfying $\langle\Psi_0|\Phi_0\rangle \neq 0$.

In DMC the Schrödinger equation is rewritten in imaginary time,

$$\frac{\partial|\psi\rangle}{\partial\tau} = -\hat{H}|\psi\rangle, \quad (2)$$

where the wave function $|\psi\rangle$ is expanded over all eigenstates of the Hamiltonian

$$|\psi\rangle = \sum_{i=0} c_i|\phi_i\rangle, \quad (3)$$

where

$$\hat{H}|\phi_i\rangle = \epsilon_i|\phi_i\rangle. \quad (4)$$

In real space, any initial state $|\psi\rangle$, that is not orthogonal to the ground state $|\phi_0\rangle$, will evolve to the ground state in the long-time limit

$$\lim_{\tau\to\infty} \psi(\mathbf{R},\tau) = c_0 e^{-\epsilon_0\tau}\phi_0(\mathbf{R}). \quad (5)$$

The long limit can be kept finite by introducing an offset $E_T = \epsilon_0$ and the Hamiltonian is separated into the kinetic energy and potential terms, leading to the diffusion form of the previous equation:

$$\frac{\partial\psi(\mathbf{R},\tau)}{\partial\tau} = \left[\sum_{i=1}^{N}\frac{1}{2}\nabla_i^2\psi(\mathbf{R},\tau)\right] - [V(\mathbf{R}) - E_T]\psi(\mathbf{R},\tau). \quad (6)$$

Since the potential $V(\mathbf{R})$ is unbounded in Coulombic systems leading to the possible divergence of the rate term $V(\mathbf{R}) - E_T$, we use importance sampling for efficiency. We introduce a trial or guiding wave function, $\psi_G(\mathbf{R})$, approximating the ground-state wave function

$$f(\mathbf{R},\tau) = \psi_G(\mathbf{R})\psi(\mathbf{R},\tau), \quad (7)$$

which is also a solution of the diffusion equation when $\psi(\mathbf{R},\tau)$ is a solution of the Schrödinger equation.

Eq. 6 becomes

$$\begin{aligned}\frac{\partial f(\mathbf{R},\tau)}{\partial\tau} = &\left[\sum_{i=1}^{N}\frac{1}{2}\nabla_i^2 f(\mathbf{R},\tau)\right]\\ &-\nabla\left[\frac{\nabla\psi(\mathbf{R})}{\psi(\mathbf{R})}f(\mathbf{R},\tau)\right]\\ &-[E_L(\mathbf{R}) - E_T]f(\mathbf{R},\tau),\end{aligned} \quad (8)$$

where E_T is a "trial energy" introduced to maintain normalization of the projected solution at large τ and E_L is a "local energy" depending on configuration $\{\mathbf{R}\}$:

$$E_L(\mathbf{R}) = \frac{\hat{H}\psi_T(\mathbf{R})}{\psi_T(\mathbf{R})}. \quad (9)$$

To maintain the fermionic nature of the wave function we impose antisymmetry to the guiding function, also known as the fixed-node approximation [51]. This approximation is variational: the accuracy of DMC depends solely on the quality of the nodes of the trial wave function and the fixed-node DMC energy is an upper bound to the exact ground-state energy. In order to remove the chemically inert core electrons, nonlocal pseudopotentials are introduced and evaluated in DMC using T-moves [37].

In contrast, AFQMC is usually formulated as an orbital-space approach in which the Hamiltonian is written as

$$\begin{aligned}\hat{H} &= \sum_{ij\sigma} h_{ij}\hat{c}_{i\sigma}^{\dagger}\hat{c}_{j\sigma} + \frac{1}{2}\sum_{ijkl,\sigma,\sigma'} v_{ijkl}\hat{c}_{i\sigma}^{\dagger}\hat{c}_{j\sigma'}^{\dagger}\hat{c}_{l\sigma'}\hat{c}_{k\sigma} + E_{II} \quad (10)\\ &= \hat{H}_1 + \hat{H}_2 + E_{II}, \quad (11)\end{aligned}$$

where $\hat{c}_{i\sigma}^{\dagger}$ and $\hat{c}_{i\sigma'}$ are the fermionic creation and annihilation operators, h_{ij} and v_{ijkl} are the one- and two-electron matrix elements, and the constant E_{II} is the ion-ion repulsion energy. The two-body part of the propagator is then written as an integral over auxiliary fields of one-body propagators using the Hubbard-Stratonovich transformation [52]. An AFQMC simulation then proceeds by sampling an instance of this propagator and applying it to a random walker which is defined by a weight and Slater determinant. Unfortunately, for the many-electron Hamiltonian the propagator will be in general complex, thus giving rise to a phase problem [9].

To control this phase problem Zhang and Krakauer introduced the phaseless-AFQMC method (ph-AFQMC) [9] which uses an importance sampling transformation and a trial wave function to enforce a constraint on the walkers' propagation. With this approximation ph-AFQMC has been applied to a wide variety of chemical [10,53–58] and solid-state [12,14,26,59] problems. For problems where static correlation is important, multireference expansions can be employed, such as complete active space self-consistent field [57,60], selected configuration interaction-based approaches [60–62], or nonorthogonal multi-Slater determinant expansions [63–66].

In this work we attempt to remove the fixed-node and phaseless error in DMC and AFQMC, respectively, by employing multideterminant trial wave functions of the form

$$|\Psi_T\rangle = \sum_I c_I |D_I\rangle, \tag{12}$$

where $|D_I\rangle$ are a set of orthogonal Slater determinants. Multideterminant expansions allow us to systematically approach the exact ground-state wave function in a finite basis set. In the limit that the exact ground-state wave function is used, AFQMC is exact in that basis set while the fixed node error will be substantially reduced. This approach allows us to systematically remove fixed node or phaseless error separately of any finite basis-set errors.

The expansion is built using CIPSI (configuration interaction using a perturbative selection made iteratively), a selected configuration interaction (CI) method introduced a long time ago by Huron *et al.* [67]. In this approach, the CI expansion is built iteratively by selecting at each step some determinants not present in the current variational space based on their estimated contribution to the full CI wave function. More precisely, denoting $|\Psi_0^{(n)}\rangle$ the CIPSI wave function at iteration n (starting, e.g., with the Hartree-Fock determinant at $n = 0$)

$$\big|\Psi_0^{(n)}\big\rangle = \sum_I c_I^{(n)} |D_I\rangle, \tag{13}$$

the perturbative contribution at first order to the wave function of each external determinant $|D_\alpha^{(n)}\rangle$ (i.e., not belonging to the variational space at this iteration and verifying $\langle D_\alpha^{(n)}|H|\Psi_0^{(n)}\rangle \neq 0$) can be quantified using their energy contribution

$$e_\alpha^{(n)} = \frac{\big|\big\langle\Psi_0^{(n)}\big|H\big|D_\alpha^{(n)}\big\rangle\big|^2}{E_{var}^{(n)} - \big\langle D_\alpha^{(n)}\big|\hat{H}\big|D_\alpha^{(n)}\big\rangle}, \tag{14}$$

where $E_{var}^{(n)}$ is the CIPSI variational energy of the wave function at this iteration

$$E_{var}^{(n)} = \frac{\big\langle\Psi_0^{(n)}\big|H\big|\Psi_0^{(n)}\big\rangle}{\big\langle\Psi_0^{(n)}\big|\Psi_0^{(n)}\big\rangle}. \tag{15}$$

In a first step, a number of external determinants corresponding to the greatest values of $e_\alpha^{(n)}$ are incorporated into the variational space and the Hamiltonian is diagonalized to give $|\Psi_0^{(n+1)}\rangle$ and $E_{var}^{(n+1)}$. In practice, the number of selected external determinants is chosen so that the size of the variational wave function is roughly doubled at each iteration. In the second step, the second-order Epstein-Nesbet energy correction to the variational energy (denoted as $E_{\text{PT2}}^{(n)}$) is computed by summing up the contributions of all external determinants

$$E_{\text{PT2}}^{(n)} = \sum_\alpha e_\alpha^{(n)}, \tag{16}$$

and the total CIPSI energy is given by

$$E_{\text{CIPSI}}^{(n)} = E_{var}^{(n)} + E_{\text{PT2}}^{(n)}. \tag{17}$$

The algorithm is then iterated until some convergence criterion (e.g., $|E_{\text{PT2}}^{(n)}| \leqslant \epsilon$) is met. For simplicity, in what follows the superscript n will be dropped from the various quantities.

As the number of selected determinants increases, higher-order perturbational contributions become smaller and the CIPSI energy can be used as an estimate of the full CI energy, E_{FCI}. To do that in practice, we have adopted the method recently proposed by Holmes *et al.* [62] in the context of the semistochastic heat-bath configuration interaction method. While increasing the number of selected determinants, the CIPSI variational energy, E_{var}, is plotted as a function of the second-order Epstein-Nesbet energy E_{PT2}. For sufficiently large expansions, $E_{var} \approx E_{FCI} - E_{\text{PT2}}$ and the extrapolated value of E_{var} at $E_{\text{PT2}} = 0$ is an estimate of the FCI limit. This extrapolation procedure has been shown to be robust, even for challenging chemical situations [61,68–73]. In what follows, these extrapolated CIPSI results are labeled exFCI.

Computational details. All the QMC calculations were performed with the development version of QMCPACK [23,24]. PYSCF [74] was used to run the DFT simulations and to generate the one- and two-electron integrals within the B3LYP [75–78] exchange and correlation functional. All calculations were carried out using the correlation-consistent effective core potentials [79–81] and the associated basis sets. The subsequent CIPSI and AFQMC simulations were performed in the molecular orbital basis. We studied three simple solids in their primitive cells: carbon in the diamond structure (two atoms per cell), lithium fluoride (two atoms per cell), and fcc aluminum (four atoms per cell), each at their experimental lattice parameters of 3.567, 4.0351, and 4.046 Å, respectively.

All CIPSI calculations were performed with QUANTUM PACKAGE [82]. The iterative process of selection was stopped when the change in $E_{var} + E_{\text{PT2}}$ between iteration n and iteration $n + 1$ varies with less than 0.5×10^{-4} Ha. Total energies of all three materials with regard to the basis-set size, final number of determinants, and value of E_{PT2} are given in the Supplemental Material [83]. The exFCI estimates obtained by extrapolation using E_{PT2} values as explained above are also reported [83].

All DMC calculations used individual Slater-Jastrow trial wave functions with one-body, two-body, and three-body Jastrow functions. The total number of determinants used in the trial wave function in the DMC runs is explicitly stated in the Supplemental Material [83]. The size of the determinant expansion corresponds to truncations using the weight of the coefficients (10^{-4}, 10^{-5}, 10^{-6}, and 10^{-8}) as an inclusion criterion. The total number of determinants spanned from 15k determinants for the LiF system in its cc-pvDz basis set to 10.5M determinants for aluminum in its cc-pvQz basis sets. The 50 parameters of the Jastrow functions were optimized

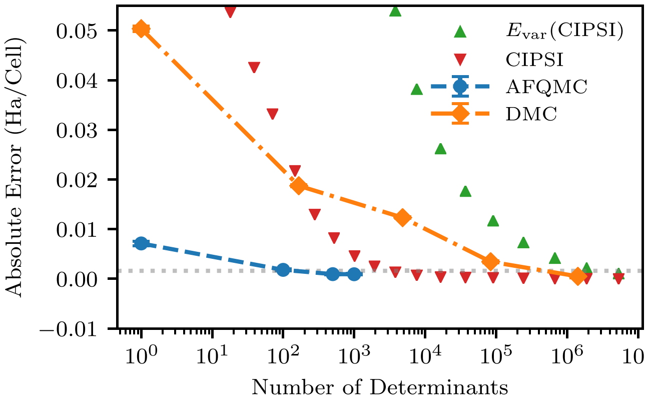

FIG. 1. Convergence of the phaseless AFQMC and fixed-node DMC error in the total energy for diamond structure carbon in the cc-pVTZ basis set with the size of the multideterminant expansion. For AFQMC the error was computed relative to CIPSI total energy in the same basis set. For DMC the error was computed with respect to the DMC result with $N_D = 1 \times 10^7$. Horizontal dashed line represents chemical accuracy of 1.6 mHa/cell. E_{var}(CIPSI) is the variational energy of the CIPSI wave function, while the full CIPSI energy includes the second-order perturbation theory correction.

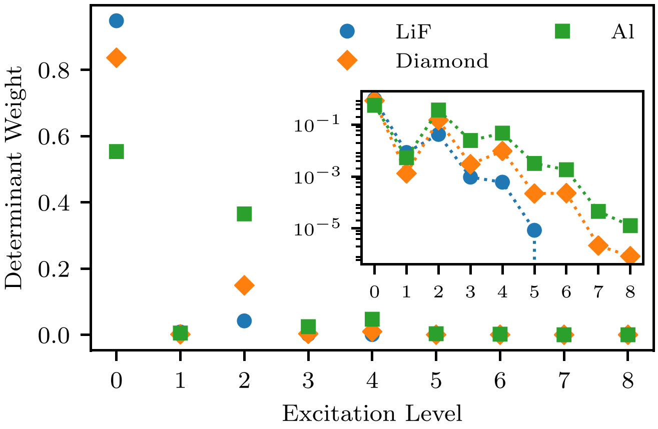

FIG. 2. Comparison in the amount of configurational weight in the CIPSI trial wave functions at each excitation level above the reference determinant in the cc-pVQZ basis set. The basis-set dependence of the determinant weight is relatively weak. Inset shows the same data on a semilogarithmic plot.

within variational Monte Carlo with a variant of the linear method of Umrigar and co-workers [84] for each system at each determinant truncation and each basis-set size. The optimized trial wave function was then used in DMC, using a 0.001 time step and 32 000 walkers.

The AFQMC simulations used a time step of 0.005 Ha^{-1}, with a population of 1440 walkers. The pair-branch population control method was used [85]. We used the modified-Cholesky decomposition [86–88] to factorize the two-electron integrals and used a convergence threshold of 1×10^{-5}. Further simulation details and convergence studies are in the Supplemental Material [83].

All input files, output data, and scripts necessary to generate the results presented are available at Ref. [89]. Note that neither the determinant coefficients nor the orbitals were reoptimized after the initial DFT and CIPSI procedure for either DMC or AFQMC, which could accelerate convergence.

Results.

In Fig. 1 we show the results for carbon (diamond) in the cc-pVXZ basis sets, where X is the cardinality of the basis set. Both AFQMC and DMC energies converge faster than the CIPSI variational energy. The phaseless error of AFQMC converges faster compared to the fixed-node error in DMC. We see that the ph-AFQMC result is within 1 mHa of the converged total energy using approximately 100 determinants. In contrast the CIPSI variational energy required $O(10^7)$ determinants to reach this level of accuracy and $O(10^4)$ determinants for the CIPSI energy. Note that reducing the number of determinants by three orders of magnitude when passing from the variational to the full CIPSI energy illustrates how much the second-order energy correction E_{PT2} is efficient at enhancing the convergence. We see that DMC also converges systematically with the size of the multideterminant expansion, although it requires $O(10^6)$ determinants to reach the same level of accuracy as AFQMC. We observed the same trends observed in carbon as in aluminum and lithium fluoride [83].

Figure 3 presents the fraction of correlation energy captured by each method relative to the estimated exact correlation energy for each material. The exact correlation energies can be obtained here with CIPSI since the regime where energies are converged both as a function of the number of determinants for a given basis set (extrapolation to $E_{\mathrm{PT2}} = 0$ to get exFCI estimates as explained above) and of the basis set (CBS limit) can be attained for these simple systems [90]. We estimate the basis-set extrapolation errors to be of the order of 1–2 mHa/cell. These are most pronounced in the case of LiF and Al. Thus, AFQMC and DMC may agree better if larger, augmented, or more optimally chosen basis sets were used, since less extrapolation would be required. We note that using a plane-wave basis could also allow for a more direct convergence of the CIPSI or AFQMC results with respect to the basis-set size. However, the plane-wave cutoffs necessary to resolve the electron-electron cusp would likely result in much larger basis sets and make the calculations more computationally demanding [91]. Details of the extrapolation are given in the Supplemental Material.

We define the percentage of correlation energy recovered as

$$\%\ \mathrm{ofcorrelationenergy} = 100 \times \left|\frac{E_c(\mathrm{QMC})}{E_c(\mathrm{exact})}\right|, \qquad (18)$$

where the correlation energy is defined as $E_c = E - E_{\mathrm{HF}}$ where E_{HF} is the restricted Hartree-Fock total energy in the CBS limit. We see that the relative gain in correlation energy by using a modest multiple determinant trial in AFQMC is small (on the order of a few percent), while the largest error from the CBS-limit exFCI results is, unsurprisingly, the basis-set error. Notably we see for LiF the phaseless error is essentially zero, and is largest in the four-atom cell of Al. The DMC results in contrast show a much larger dependence on trial wave function, with the single-determinant correlation energies exhibiting up to a 20% error. In the smallest tested basis (double zeta), DMC is always more accurate for total

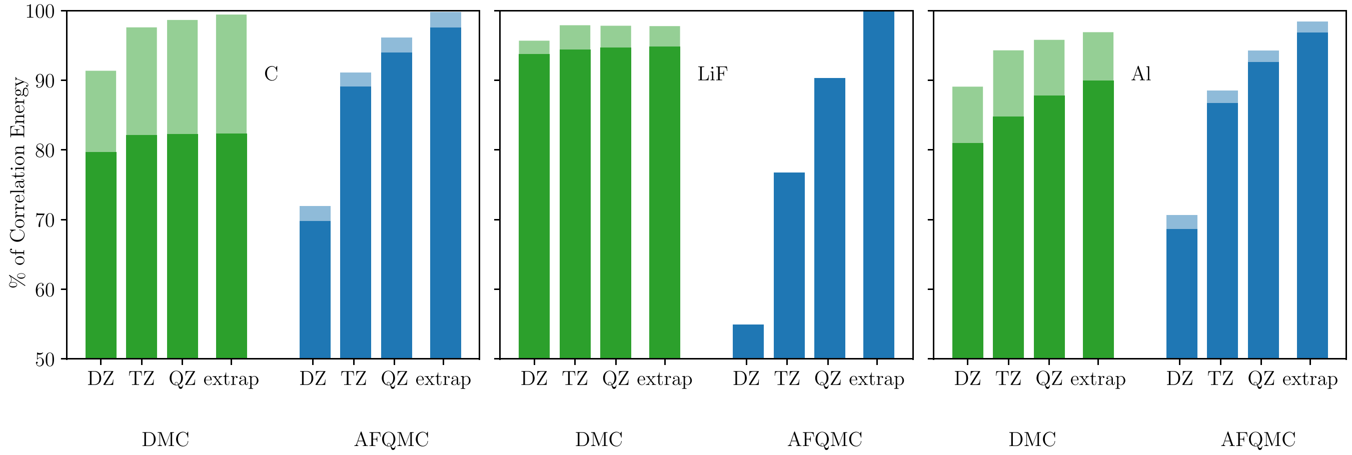

FIG. 3. Comparison between the amount of correlation energy captured by DMC and AFQMC with single-determinant (dark bars) and multideterminant (light bars) trial wave functions for unit cells of carbon (diamond), LiF, and Al. For both DMC and AFQMC we compare to the converged CBS-limit exFCI correlation energies computed with CIPSI.

energies than AFQMC performed in the same basis. However, the DMC improves slowly with multiple determinants and with increased basis-set size, while the accuracy of AFQMC gains rapidly. Table I summarizes our results for single determinants and for the largest number of determinants that were run for each material.

For the case of aluminum we begin to see the ultimate limitation of all methods to systematically remove their respective constraint error. Obtaining a reliable estimate of exFCI correlation energies was challenging, due to the difficulty in reaching the linear regime, $E_{var} \approx E_{FCI} - E_{\mathrm{PT2}}$, required for the extrapolation step [83]. While in the case of AFQMC, we found it challenging to reach the same level of convergence in the cc-pVQZ basis set as in the cc-pVDZ basis set, due to the computational cost which grows with the basis-set size. Thus, the CBS extrapolated AFQMC value in this case is not fully reliable.

To gain further insight into the relative rate of convergence of DMC and AFQMC with the number of determinants for different systems, we plot in Fig. 2 the configurational weight at each excitation level in the trial wave function for the systems considered in the cc-pVQZ basis set. We see that the multireference character of the wave function increases as we move from LiF to Al. LiF is dominated by single and double excitations, while triples and quadruple excitations become more relevant for diamond and aluminum. The aluminum wave function in particular has significant doubles contributions (≈36%) and non-negligible contributions up to sextuple excitations. This trend in increasing multireference character maps well onto the magnitude of the phaseless error seen in Fig. 3.

TABLE I. Converged CIPSI total (E), Hartree-Fock (E_{HF}), and correlation E_c energies for the systems considered here. Also presented is the error in the basis-set extrapolated AFQMC and DMC correlation energies. Energies are in Hartree/cell. SD indicates single-determinant results while MD indicates results from the largest multideterminant trial wave functions for each system.

	C	LiF	Al
E_{HF}	−10.2381	−31.5559	−7.7987
E	−10.5569	−31.9038	−8.2158
E_c	−0.3187	−0.3479	−0.4171
AFQMC(SD)	−0.0077(9)	0.0008(5)	−0.0130(8)
AFQMC(MD)	−0.0007(3)	−0.0008(7)	−0.0067(6)
DMC(SD)	−0.0563(8)	−0.0180(8)	−0.042(1)
DMC(MD)	−0.002(2)	−0.008(2)	−0.0129(8)

This increased multireference character coupled with the larger number of electrons makes aluminum more challenging to converge for all methods and shows the limitation of the present multideterminant trial wave functions. This is perhaps unsurprising as we would expect that the amount of correlation energy captured for a fixed multideterminant size should decay exponentially with system size. Nevertheless, for these relatively simple cases, we managed to obtain reliably converged total energies accurate to roughly 1–2 mHa/cell, which should serve as useful benchmarks for future studies.

Discussion and conclusions. We have shown it possible to systematically converge CIPSI, AFQMC, and DMC to the exact ground-state total energy of three simple finite-size solids. We have shown that the phaseless constraint in AFQMC is often much smaller than the fixed-node error in DMC, an observation that has not been quantified before in solids. We also showed that the phaseless error can be removed by using smaller multideterminant expansions than DMC. At the same time we found that AFQMC exhibits a much larger basis-set error than DMC.

In light of these findings it is clear that the most important issues for the application of AFQMC in solids is the development of robust basis-set correction techniques to accelerate convergence and the development of optimized basis sets. For DMC it is the need to develop more accurate compact trial wave functions that converge similarly efficiently as in AFQMC. This could be via optimized orbitals and improved multiple determinant selection schemes, a full reoptimization of determinant coefficients, or wholly different wave functions such as Geminals, Pfaffians, or backflow. For practical applications where relative energies rather than total energies are used, convergence of both methods is likely to be better due to cancellation of errors. Indeed, cohesive energies computed from single-determinant DMC are often very accurate [16–19]. Further work should investigate why single-determinant DMC errors are so large by, for example, investigating the magnitude of the locality error.

Looking to the future, an important topic not addressed is the treatment of finite-size effects [92]. In light of our findings, it seems highly unlikely that highly converged multideterminant trial wave functions could be used to obtain thermodynamic limit total energies in QMC. Nevertheless, it may be possible to obtain corrections using simpler wave functions, and apply this correction to more accurate small unit-cell results [92]. Interestingly, we found that the phaseless error in AFQMC is roughly independent of the basis-set size [83]. Further work should include the investigation of a more diverse set of materials under the effects of strain or doping, the effect of basis set and orbital optimizations, and the convergence of properties other than the total energy with respect to the trial wave function. Ultimately, we hope that our results will serve as helpful reference and motivate the development of compact and efficient trial wave functions for both AFQMC and DMC.

The Department of Energy will provide public access to these results of federally sponsored research in accordance with the DOE Public Access Plan [93].

Acknowledgments. This work has been partially supported by U.S. DOE. ORNL is managed by UT-Battelle, LLC, under Contract No. DE-AC05-00OR22725 for the U.S. Department of Energy. The U.S. Government retains and the publisher, by accepting the article for publication, acknowledges that the United States Government retains a nonexclusive, paid-up, irrevocable, worldwide license to publish or reproduce the published form of this manuscript or allows others to do so for U.S. Government purposes. This work was supported by the U.S. Department of Energy (DOE), Office of Science, Basic Energy Sciences, Materials Sciences and Engineering Division, as part of the Computational Materials Sciences Program and Center for Predictive Simulation of Functional Materials (CPSFM). M.C. was supported by the ANR PhemSpec project, Grant No. ANR-18-CE30-0025-02 of the French Agence Nationale de la Recherche, and A.B. and M.C. were partially supported by the international exchange program CNRS-PICS, France-USA. An award of computer time was provided by the Innovative and Novel Computational Impact on Theory and Experiment (INCITE) program. All CIPSI and DMC calculations used resources of the Argonne Leadership Computing Facility, which is a DOE Office of Science User Facility supported under Contract No. DE-AC02-06CH11357. AFQMC calculations received computing support from the LLNL Institutional Computing Grand Challenge program. The work of F.D.M. and M.A.M. was performed under the auspices of the U.S. DOE by LLNL under Contract No. DE-AC52-07NA27344. Sandia National Laboratories is a multimission laboratory managed and operated by National Technology and Engineering Solutions of Sandia, LLC, a wholly owned subsidiary of Honeywell International Inc., for the U.S. Department of Energy's National Nuclear Security Administration under Contract No. DE-NA0003525.

---

[1] P. R. C. Kent and G. Kotliar, Science **361**, 348 (2018).
[2] P. Hohenberg and W. Kohn, Phys. Rev. B **136**, 864 (1964).
[3] W. Kohn and L. J. Sham, Phys. Rev. A **140**, 1133 (1965).
[4] M. G. Medvedev, I. S. Bushmarinov, J. Sun, J. P. Perdew, and K. A. Lyssenko, Science **355**, 49 (2017).
[5] E. A. Carter, Science **321**, 800 (2008).
[6] G. H. Booth, A. Grüneis, G. Kresse, and A. Alavi, Nature (London) **493**, 365 (2013).
[7] W. M. C. Foulkes, L. Mitas, R. J. Needs, and G. Rajagopal, Rev. Mod. Phys. **73**, 33 (2001).
[8] S. Zhang, J. Carlson, and J. E. Gubernatis, Phys. Rev. B **55**, 7464 (1997).
[9] S. Zhang and H. Krakauer, Phys. Rev. Lett. **90**, 136401 (2003).
[10] M. Motta and S. Zhang, WIREs Comput. Mol. Sci. **8**, e1364 (2018).
[11] J. P. F. LeBlanc *et al.*, Phys. Rev. X **5**, 041041 (2015).
[12] M. Motta, D. M. Ceperley, Garnet Kin-Lic Chan, J. A. Gomez, E. Gull, S. Guo, C. A. Jimenez-Hoyos, T. N. Lan, J. Li, F. Ma, A. J. Millis, N. V. Prokofev, U. Ray, G. E. Scuseria, S. Sorella, E. M. Stoudenmire, Q. Sun, I. S. Tupitsyn, S. R. White, D. Zgid, and S. Zhang, Phys. Rev. X **7**, 031059 (2017).
[13] K. T. Williams *et al.*, Phys. Rev. X **10**, 011041 (2020).
[14] S. Zhang, F. D. Malone, and M. A. Morales, J. Chem. Phys. **149**, 164102 (2018).
[15] J. Lee, F. D. Malone, and M. A. Morales, J. Chem. Theory Comput. **16**, 3019 (2020).
[16] K. Saritas, J. T. Krogel, and F. A. Reboredo, Phys. Rev. B **98**, 155130 (2018).
[17] M. Dubecký, L. Mitas, and P. Jurečka, Chem. Rev. **116**, 5188 (2016).
[18] J. A. Santana, J. T. Krogel, P. R. C. Kent, and F. A. Reboredo, J. Chem. Phys. **144**, 174707 (2016).
[19] K. P. Driver, R. E. Cohen, Z. Wu, B. Militzer, P. L. Rios, M. D. Towler, R. J. Needs, and J. W. Wilkins, Proc. Natl. Acad. Sci. USA **107**, 9519 (2010).
[20] N. Devaux, M. Casula, F. Decremps, and S. Sorella, Phys. Rev. B **91**, 081101(R) (2015).
[21] G. Ferlat, M. Hellgren, F.-X. Coudert, H. Hay, F. Mauri, and M. Casula, Phys. Rev. Mater. **3**, 063603 (2019).
[22] M. Casula and S. Sorella, Phys. Rev. B **88**, 155125 (2013).
[23] J. Kim *et al.*, J. Phys.: Condens. Matter **30**, 195901 (2018).
[24] P. R. C. Kent *et al.*, J. Chem. Phys. **152**, 174105 (2020).
[25] J. Carlson, J. E. Gubernatis, G. Ortiz, and S. Zhang, Phys. Rev. B **59**, 12788 (1999).
[26] M. Suewattana, W. Purwanto, S. Zhang, H. Krakauer, and E. J. Walter, Phys. Rev. B **75**, 245123 (2007).
[27] F. Ma, S. Zhang, and H. Krakauer, Phys. Rev. B **95**, 165103 (2017).
[28] F. Ma, W. Purwanto, S. Zhang, and H. Krakauer, Phys. Rev. Lett. **114**, 226401 (2015).

[29] W. Purwanto, S. Zhang, and H. Krakauer, J. Chem. Theory Comput. **9**, 4825 (2013).

[30] F. D. Malone, S. Zhang, and M. A. Morales, J. Chem. Theory. Comput. **15**, 256 (2019).

[31] M. Motta, S. Zhang, and Garnet Kin-Lic Chan, Phys. Rev. B **100**, 045127 (2019).

[32] C.-C. Chang, B. M. Rubenstein, and M. A. Morales, Phys. Rev. B **94**, 235144 (2016).

[33] R. Q. Hood, P. R. C. Kent, and F. A. Reboredo, Phys. Rev. B **85**, 134109 (2012).

[34] Y. Luo, A. Benali, L. Shulenburger, J. T. Krogel, O. Heinonen, and P. R. C. Kent, New J. Phys. **18**, 113049 (2016).

[35] J. A. Santana, J. T. Krogel, S. Okamoto, and F. A. Reboredo, J. Chem. Theory Comput. **16**, 643 (2019).

[36] L. Mitas, E. L. Shirley, and D. M. Ceperley, J. Chem. Phys. **95**, 3467 (1991).

[37] M. Casula, S. Moroni, S. Sorella, and C. Filippi, J. Chem. Phys. **132**, 154113 (2010).

[38] P. Rosenberg, H. Shi, and S. Zhang, Phys. Rev. Lett. **119**, 265301 (2017).

[39] E. G. Hohenstein, R. M. Parrish, and T. J. Martínez, J. Chem. Phys. **137**, 044103 (2012).

[40] R. M. Parrish, E. G. Hohenstein, T. J. Martínez, and C. D. Sherrill, J. Chem. Phys. **137**, 224106 (2012).

[41] E. G. Hohenstein, R. M. Parrish, C. D. Sherrill, and T. J. Martínez, J. Chem. Phys. **137**, 221101 (2012).

[42] J. Lu and L. Ying, J. Comput. Phys. **302**, 329 (2015).

[43] W. Hu, L. Lin, and C. Yang, J. Chem. Theory Comput. **13**, 5420 (2017).

[44] K. Dong, W. Hu, and L. Lin, J. Chem. Theory Comput. **14**, 1311 (2018).

[45] M. Motta, J. Shee, S. Zhang, and G. K.-L. Chan, J. Chem. Theory Comput. **15**, 3510 (2019).

[46] M. Motta and S. Zhang, J. Chem. Theory Comput. **13**, 5367 (2017).

[47] M. Motta, D. E. Galli, S. Moroni, and E. Vitali, J. Chem. Phys. **140**, 024107 (2014).

[48] M. Motta, D. E. Galli, S. Moroni, and E. Vitali, J. Chem. Phys. **143**, 164108 (2015).

[49] E. Vitali, H. Shi, M. Qin, and S. Zhang, Phys. Rev. B **94**, 085140 (2016).

[50] M. Motta and S. Zhang, J. Chem. Phys. **148**, 181101 (2018).

[51] J. B. Anderson, J. Chem. Phys. **65**, 4121 (1976).

[52] J. Hubbard, Phys. Rev. Lett. **3**, 77 (1959).

[53] W. A. Al-Saidi, H. Krakauer, and S. Zhang, Phys. Rev. B **73**, 075103 (2006).

[54] W. Purwanto, H. Krakauer, Y. Virgus, and S. Zhang, J. Chem. Phys. **135**, 164105 (2011).

[55] W. Purwanto, S. Zhang, and H. Krakauer, J. Chem. Phys. **142**, 064302 (2015).

[56] J. Shee, B. Rudshteyn, E. J. Arthur, S. Zhang, D. R. Reichman, and R. A. Friesner, J. Chem. Theory Comput. **15**, 2346 (2019).

[57] J. Shee, S. Zhang, D. R. Reichman, and R. A. Friesner, J. Chem. Theory Comput. **13**, 2667 (2017).

[58] H. Hao, J. Shee, S. Upadhyay, C. Ataca, K. D. Jordan, and B. M. Rubenstein, J. Phys. Chem. Lett. **9**, 6185 (2018).

[59] J. Lee, F. D. Malone, and M. A. Morales, J. Chem. Phys. **151**, 064122 (2019).

[60] W. Purwanto, S. Zhang, and H. Krakauer, J. Chem. Phys. **130**, 094107 (2009).

[61] S. Sharma, A. A. Holmes, G. Jeanmairet, A. Alavi, and C. J. Umrigar, J. Chem. Theory Comput. **13**, 1595 (2017).

[62] A. A. Holmes, N. M. Tubman, and C. J. Umrigar, J. Chem. Theory Comput. **12**, 3674 (2016).

[63] C. A. Jiménez-Hoyos, R. Rodríguez-Guzmán, and G. E. Scuseria, J. Chem. Phys. **139**, 204102 (2013).

[64] R. Schutski, C. A. Jiménez-Hoyos, and G. E. Scuseria, J. Chem. Phys. **140**, 204101 (2014).

[65] C. A. Jiménez-Hoyos, T. M. Henderson, T. Tsuchimochi, and G. E. Scuseria, J. Chem. Phys. **136**, 164109 (2012).

[66] E. J. Landinez Borda, J. Gomez, and M. A. Morales, J. Chem. Phys. **150**, 074105 (2019).

[67] B. Huron, J. P. Malrieu, and P. Rancurel, J. Chem. Phys. **58**, 5745 (1973).

[68] A. A. Holmes, C. J. Umrigar, and S. Sharma, J. Chem. Phys. **147**, 164111 (2017).

[69] A. Scemama, Y. Garniron, M. Caffarel, and P. F. Loos, J. Chem. Theory Comput. **14**, 1395 (2018).

[70] A. Scemama, A. Benali, D. Jacquemin, M. Caffarel, and P. F. Loos, J. Chem. Phys. **149**, 034108 (2018).

[71] A. D. Chien, A. A. Holmes, M. Otten, C. J. Umrigar, S. Sharma, and P. M. Zimmerman, J. Phys. Chem. A **122**, 2714 (2018).

[72] Y. Garniron, A. Scemama, E. Giner, M. Caffarel, and P. F. Loos, J. Chem. Phys. **149**, 064103 (2018).

[73] P. F. Loos, A. Scemama, A. Blondel, Y. Garniron, M. Caffarel, and D. Jacquemin, J. Chem. Theory Comput. **14**, 4360 (2018).

[74] Q. Sun, T. C. Berkelbach, N. S. Blunt, G. H. Booth, S. Guo, Z. Li, J. Liu, J. D. McClain, E. R. Sayfutyarova, S. Sharma, S. Wouters, and G. K. L. Chan, WIREs Comput. Mol. Sci. **8**, e1340 (2017).

[75] A. D. Becke, J. Chem. Phys. **98**, 5648 (1993).

[76] C. Lee, W. Yang, and R. G. Parr, Phys. Rev. B **37**, 785 (1988).

[77] S. H. Vosko, L. Wilk, and M. Nusair, Can. J. Phys. **58**, 1200 (1980).

[78] P. J. Stephens, F. J. Devlin, C. F. Chabalowski, and M. J. Frisch, J. Phys. Chem. **98**, 11623 (1994).

[79] M. C. Bennett, G. Wang, A. Annaberdiyev, C. A. Melton, L. Shulenburger, and L. Mitas, J. Chem. Phys. **149**, 104108 (2018).

[80] M. C. Bennett, C. A. Melton, A. Annaberdiyev, G. Wang, L. Shulenburger, and L. Mitas, J. Chem. Phys. **147**, 224106 (2017).

[81] G. Wang, A. Annaberdiyev, C. A. Melton, M. C. Bennett, L. Shulenburger, and L. Mitas, J. Chem. Phys. **151**, 144110 (2019).

[82] Y. Garniron, T. Applencourt, K. Gasperich, A. Benali, A. Ferté, J. Paquier, B. Pradines, R. Assaraf, P. Reinhardt, J. Toulouse, P. Barbaresco, N. Renon, G. David, J.-P. Malrieu, M. Véril, M. Caffarel, P.-F. Loos, E. Giner, and A. Scemama, J. Chem. Theory Comput. **15**, 3591 (2019).

[83] See Supplemental Material at http://link.aps.org/supplemental/10.1103/PhysRevB.102.161104 for raw QMC and CIPSI energies along with more detailed convergence studies.

[84] C. J. Umrigar, J. Toulouse, C. Filippi, S. Sorella, and R. G. Hennig, Phys. Rev. Lett. **98**, 110201 (2007).

[85] L. K. Wagner, M. Bajdich, and L. Mitas, J. Comput. Phys. **228**, 3390 (2009).

[86] N. H. F. Beebe and J. Linderberg, Int. J. Quantum Chem. **12**, 683 (1977).

[87] H. Koch, A. S. de Merás, and T. B. Pedersen, J. Chem. Phys. **118**, 9481 (2003).

[88] F. Aquilante, L. De Vico, N. Ferré, G. Ghigo, P. Malmqvist, P. Neogrády, T. B. Pedersen, M. Pitoňák, M. Reiher, B. O. Roos, L. Serrano-Andrés, M. Urban, V. Veryazov, and R. Lindh, J. Comput. Chem. **31**, 224 (2009).

[89] All simulation data is available at https://doi.org/10.18126/bbh5-icx2.

[90] T. Helgaker, W. Klopper, H. Koch, and J. Noga, J. Chem. Phys. **106**, 9639 (1997).

[91] J. J. Shepherd, A. Grüneis, G. H. Booth, G. Kresse, and A. Alavi, Phys. Rev. B **86**, 035111 (2012).

[92] A. Benali, K. Gasperich, K. D. Jordan, T. Applencourt, Y. Luo, M. C. Bennett, J. T. Krogel, L. Shulenburger, P. R. Kent, P.-F. Loos *et al.*, arXiv:2007.11673.

[93] http://energy.gov/downloads/doe-public-access-plan.